Optimal allocation of Prognostics and Health Management capabilities to improve the reliability of a power transmission network

Michele Compare[1,2], Luca Bellani[1,2], Enrico Zio[1,2,3,*]

[1]Energy Department, Politecnico di Milano, Italy

[2]Aramis S.r.l., Italy

[3]Chair on Systems Science and the Energetic challenge, Foundation Electricité de France at CentraleSupélec, France

[*]corresponding author; enrico.zio@polimi.it

Abstract

We introduce a new perspective to improve the reliability of a network, which aims at finding cost-effective portfolios of Prognostics and Health Management (PHM) systems to be installed throughout the network. To do this, we estimate the reliability of the single network element equipped with a PHM system, whose prognostic performance is measured in terms of the $\alpha-\lambda$ performance, false positive and false negative metrics. Then, we apply genetic algorithms for finding the portfolios of PHM systems to be installed on the network elements, which are optimal with respect to cost and a global reliability efficiency index of the network. The workbench case study of the IEEE 14 bus network is considered as application.

Keywords: Maintenance, PHM, Portfolio Decision Analysis, Power Transmission System, Reliability Allocation

Symbols & Acronyms

α	Parameter related to the performance metrics
α_λ^+	$(1+\alpha)RUL_\lambda^*$

α_λ^-	$(1-\alpha)RUL_\lambda^*$
β	Percentile related to the maintenance criterion
Δt	Time interval between two successive Remaining Useful Life (RUL) predictions
$\gamma_{i,j}$	Path between nodes i and j, i.e., a sequence of nodes $(i_1, i_2, ..., i_k)$, $k > 1$ such that $(i_j, i_{j+1}) \in E,\ 1 \leq j < k\ , i_1 = i, i_k = j$
λ	Equivalent time indicator, such that $t_\lambda = T_{pr} + \lambda(T_f - T_{pr})$; $\lambda \in [0, 1]$
$\mathbf{z}$	Vector encoding the decision variables
$\mathcal{A}$	Set of alternative actions
$\lfloor x \rfloor$	Integer part of x; that is, $n \leq x < n+1$, $x \in \mathbb{R}$, $n \in \mathbb{N}$
$\mathcal{G}(a, b)$	Gamma distribution with shape parameter a and inverse scale parameter b; the probability density function (pdf) is $f_{\mathcal{X}}(x) = \frac{b^a x^{a-1} e^{-bx}}{\Gamma(a)}$; $\Gamma(a) = \int_0^\infty x^{a-1} e^{-x} dx$
Ω	Number of available alternative PHM systems
Υ_λ	Point summarizing the uncertainty in R_λ (e.g., mean, median, 10^{th} percentile, etc.)
B	Available budget
DTD	Detection Time Delay, $T_{pr} - T_d$
E	Set of network edges
E'	Set of indexes univocally associated to the edges in E
$E^r[G]$	Global reliability efficiency of network G
f_{DTD}	probability density function (pdf) of DTD
$f_{T_d}(t)$	pdf of time T_d
$f_{T_f}(t)$	pdf of failure time T_f
f_{T_ϕ}	Probability Density Function (pdf) of T_ϕ
FN	False Negatives
FP	False Positives
$G(V, E)$	Graph with nodes V and edges E
h	$h \cdot \Delta t$ is the time required to safely remove the component from operation

L	Quality level of the PHM systems
N	Number of maximum RUL predictions before failure
N_V	Cardinality of V, i.e. number of nodes
P_λ^α	α-λ performance
Pi_λ^α	Binary indicator of PHM prediction accuracy
$q_{m,n}(T)$	Reliability at time horizon T of the edge connecting nodes m and n
R_λ	Uncertain predicted RUL at time λ
RC_i^C	Reliability closeness centrality of node i
$rd_{i,j}$	Most reliable path between nodes i and j
RUL_λ^*	Actual RUL at the equivalent time λ
T	Time horizon
T_d	Time instant at which the system reaches the detection threshold
T_ϕ	$T_f - T_{pr}$
T_{pr}	Time of the first RUL prediction
$u_{m,n}(T)$	Unreliability at time horizon T of the edge connecting nodes m and n
V	Set of network nodes
DM	Decision Maker
GA	Genetic Algorithm

1 Introduction

In the last decades, the frequency of blackouts in electric power transmission grids has not decreased, in spite of the enhancements of the reliability standards and the significant technological advances in the field. This situation, partly due to the increase in the sizes of the grids and the growth of their interconnections and interdependences over large transnational regions [1], justifies the search by the electrical network operators of failure protection solutions that preserve the grid operation competitiveness in the deregulated market of electricity production and transmission.

For this, various approaches have been proposed, which mainly focus on the identification of effective modifications and/or expansions of the existing networks and less straining modes of their operation. To cite a few of these approaches, Cadini et al. ([2]) frame the addition of new links throughout the network as a Multi-Objective Optimization (MOO) problem, the objectives being the maximization of a proper network reliability metric and the minimization of the cost. Still in the MOO setting, Zio & Golea ([3]) address the issue of identifying the groups of elements whose reliability improvements yield the largest increment in the reliability of a large network, at minimum cost. In [4], Choi et al. focus on technical solutions for the minimization of the network expansion cost, while guaranteeing the fulfillment of a constraint on the minimum network reliability. Roos ([5]) considers two indicators, i.e., the average annual cost due to unplanned interruptions incurred by the customers of the system and the maximum annual capital, to compare a set of alternatives (e.g., technical improvements of specific parts of the network) with respect to their effect on the network reliability growth; among the best alternatives, the author selects the most profitable ones. Lågland ([6]) evaluates the impact of different fault restricting methods (i.e., extended use of feeder automation and a wider utilization of specific features of different feeder types) on reliability and costs of a power transmission system. Fang et al. ([7]) consider the problem of allocation of generation to distributors by rewiring links under the objectives of maximizing network resilience to cascading failure and minimizing investment costs. In [8], Sansavini et al. develop a framework to minimize the cascade effect due to the removal of an element of the network.

Nowadays, the optimal management of grids can benefit from the application of Prognostics and Health Management (PHM) methods to detect, diagnose, and predict failures of components and systems (see [10; 11; 12; 13; 14] for overviews). Although it seems intuitive that PHM can contribute to the improvement of the network reliability, nonetheless to the authors' best knowledge only a few works investigate how and to which extent. According to [9], this lack of research can be justified by the fact that when dealing with complex systems, it is very challenging to allocate reliability and PHM to each and every component: the effort required to solve this allocation problem with just a limited amount of resources may be laborious, time-consuming, and may end up with no-feasible-solution results.

Approaches to tackle the PHM allocation issue are proposed in [9; 15; 16], where a link between the PHM capabilities of a system and its resilience is established; this is defined as a failure probability combining the system inherent reliability and restoration capability of recovering from disruptive events. The main limitations of these works lie in that:

- the PHM performance is summarized by static metrics not related to PHM algorithm performance metrics [2; 3]), whereby the decisions about when to remove the system from operation are not dependent on time.

- Component reliability and PHM capabilities are considered independent on each other, the PHM capability intervening only if the component is failed. Indeed, PHM systems start working when the components start operating. This is a fundamental concern, as the knowledge of the Remaining Useful Life (RUL) can be exploited to operate the component at different loads, thus changing its reliability.

Moreover, the framework proposed in [15; 16] is not simply applicable to the complexity of an electrical network, whose reliability behaviour cannot be captured by the traditional reliability schemes of series and parallel systems.
This work proposes a new perspective for tackling the issue of the allocation of PHM capabilities on a complex network to improve its reliability, given a limited budget. To develop this novel PHM-based approach to network reliability, we have to consider that:

- The gain in the reliability of the network elements achieved through PHM depends on the performances in failure detection, diagnostics and prognostics ([17], [18], [19]). To establish a link between the metrics measuring these performances and the component reliability, we use the analytic model proposed in [20], which relies on time-variant PHM performance metrics. This allows overcoming the limitations of [9; 15; 16]. Then, we rely on the metrics proposed in [2; 3] to propagate the effect of the reliability gain brought by PHM at the network element level onto the increase in reliability at the overall network level.

- The PHM performance values are strongly related to the investment cost: PHM systems with better performances are usually more expensive, but also yield larger improvements in component reliability. We rely on the Portfolio Decision Analysis (PDA, [12], [21], [22]) to tackle the decision problem of selecting for every network element a PHM system among a set of a few alternatives of different performance levels and costs. PDA has proven in numerous applications to effectively support decision-makers when they are faced with alternative courses of action (i.e., the installation of a PHM system on the network elements) that, if selected, consume resources (i.e., the available budget) and lead to consequences with regard to proper case-dependent criteria (i.e., network reliability) ([21]). Obviously, the actions are interdependent, if only because they compete for the same resources.

To sum up, the main contribution of this paper lies in the new perspective proposed to approach the problem of improving the reliability and, thus, the safety of a critical infrastructure. This allows finding cost-effective solutions of allocation of PHM capabilities on the network nodes. To do this, we formalize the optimization problem within the PDA framework and use several algorithms and models available in literature. The novel PHM-based approach to network reliability is illustrated by way of the workbench case study of the transmission network system IEEE 14 BUS [23]. To

highlight the advantages of the proposed PDA approach, the results obtained are compared to those of some intuitive approaches of literature [24], [25], [26], which, however, are shown to not guarantee finding of the optimal solutions. In this respect, an additional major difference between our work and that proposed in [9] lies in that we consider the portfolio perspective to address the allocation issue, which directly allocates the PHM capabilities onto the network elements to optimize the global reliability efficiency of the network. On the contrary, in [9] the critical components of the series-parallel systems are first identified through a sensitivity analysis procedure, which, however, may not be applicable to network systems; then, the resilience of the components is increased to reach the target global resilience level. This importance-driven approach for budget allocation has proven to lead to sub-optimal results ([27]).
The remainder of the paper is as follows: Section 2 summarizes the reliability model of a PHM-equipped component proposed in [20]; Section 3 describes the metrics used to quantify the impact of PHM on the overall network reliability; Section 4 shows the PDA setting; Section 5 describes the case study network and the decision alternatives; Section 6 shows the results of the PDA approach and compares them with those of some intuitive approaches; Section 7 concludes the work.

2 Reliability model of a PHM-equipped component

In this Section, we summarize the model proposed in [20] to estimate the reliability of a degrading element (component or system) of the network, when it is equipped with PHM capabilities.
We assume that the network elements are affected by a single stochastic degradation process and that the variable representative of the degradation state, which is monitored every Δt units of time, can achieve two thresholds:

- The detection threshold, which mainly depends on the characteristics of the instrumentation used to measure the degradation variable (i.e., for values below this threshold it is not possible to detect the degradation state); it is reached at time T_d, although this achievement is detected DTD time later, due to the uncertainty in the measurement system.
- The failure threshold, above which the component function is lost; it is reached T_ϕ time after T_d, at time $T_f = T_d + T_\phi$.

In this setting, the PHM system starts to predict at time $T_{pr} = (\lfloor \frac{T_d + DTD}{\Delta t} \rfloor + 1)\Delta t$ the component or system RUL in the form of a Probability Density Function (pdf) f_{R_λ}, where $\lambda \in [0, 1]$: $t_\lambda = T_{pr} + \lambda(T_f - T_{pr})$ is an equivalent time indicator that re-scales and evens the component lives onto the $[0, 1]$ interval, whereas $\lfloor \circ \rfloor$ indicates the integer part of its argument.
With respect to the maintenance decision strategy, we assume that the PHM-equipped network

element is stopped when the $(100-\beta)^{th}$ percentile, Υ_λ (e.g., $\Upsilon_\lambda = 100-90 = 10^{th}$), of the currently predicted RUL pdf is smaller than $h \cdot \Delta t$: the larger the value of β, the smaller the value of the predicted RUL percentile, the more risk-averse the decision. Similarly, the larger the value of h, the more cautious the decision maker.

To estimate the unreliability over time of the PHM-equipped network element, the model proposed in [20] relies on the following time-variant prognostic metrics of literature ([17], [18], [19]), which are always indicated with subscript λ to highlight the dependence of their values on time:

- P_λ^α is the probability that f_{R_λ} overlaps the error band $[\alpha_\lambda^-, \alpha_\lambda^+]$ with a probability mass larger than β, being $\alpha_\lambda^- = (1-\alpha)RUL_\lambda^*$, $\alpha_\lambda^+ = (1+\alpha)RUL_\lambda^*$ and RUL_λ^* the actual RUL at equivalent time λ. Consider the binary indicator variable Π_λ^α:

$$\Pi_\lambda^\alpha = \begin{cases} 1, & \text{if } f_{R_\lambda}|_{\alpha_\lambda^-}^{\alpha_\lambda^+} \geq \beta \\ 0, & \text{else} \end{cases} \tag{1}$$

  Then, $P_\lambda^\alpha = \mathbb{E}[\Pi_\lambda^\alpha]$. In words, P_λ^α is the probability that the prognostic algorithm correctly estimates the RUL. Notice that the value of β in the definition of P_λ^α must be the same as the percentile related to the maintenance decision: as reported in Appendix B, this allows linking the P_λ^α metric to the reliability of the PHM-equipped component under the selected maintenance criteria.

- FP_λ is the probability that the prognostic algorithm makes large RUL under-estimation errors (i.e., $\Upsilon_\lambda < (1-\alpha)RUL_\lambda^*$), conditional on the event that the RUL prediction is outside the error band $[(1-\alpha)RUL_\lambda^*, (1+\alpha)RUL_\lambda^*]$.

- FN_λ is the probability that the prognostic algorithm makes large RUL over-estimation errors (i.e., $\Upsilon_\lambda > (1+\alpha)RUL_\lambda^*$), conditional on the event that the RUL prediction is outside the error band $[(1-\alpha)RUL_\lambda^*, (1+\alpha)RUL_\lambda^*]$.

Based on these considerations and assumptions, we have developed in [20] the reliability model of a PHM-equipped component with estimated values $p_\lambda^\alpha, fn_\lambda, fp_\lambda$ of metrics $P_\lambda^\alpha, FN_\lambda, FP_\lambda$, respectively. Namely, the PHM-equipped component is framed as a three-state system, the possible states being: *Working*, *Failed* and *Removed* (Figure 1); then, the component unreliability $u(t)$ represents the probability of having a transition from *Working* to *Failed* before time t:

$$u(t) = \mathbb{P}(T_f \leq t \ \cap \ \text{system not removed before } t\,; \boldsymbol{\theta}) =$$

$$\mathbb{P}(T_f \leq t \mid \text{system not removed before } t\,; \boldsymbol{\theta}) \times \mathbb{P}(\text{system not removed before } t\,; \boldsymbol{\theta})$$

where $\boldsymbol{\theta}$ indicates the parameters determining the performance of the PHM system, which the unreliability depends on.

Accordingly, in [20] we have derived $u(t)$ from the probabilistic transport kernel $K(t, Failed; \boldsymbol{\theta})$, which is defined as the probability that the component makes the next transition between t and $t + dt$ toward state $Failed$ ([28], Figure 1), provided that the component is set at $t = 0$ in state $Working$ (see Appendix B):

$$u(t) = \int_0^t K(\tau, Failed; \boldsymbol{\theta}) d\tau \tag{2}$$

Notice that this definition of unreliability contains some abuse of notation as $\lim_{t\to\infty} u(t) = \mathbb{P}(\text{system not removed before } t\ ; \boldsymbol{\theta}) \leq 1$, whereas, to be rigorous, the unreliability represents the Cumulative Distribution Function (CDF) of the failure time and, thus, tends to one as t increases ([29]).

Notice also that we call reliability the complement to 1 of $u(t)$, which represents the probability of being either in state *Working* or *Removed*: in both cases, the occurrence of failure has been avoided.

Finally, we have shown in [20] that the reliability value is more sensitive to the values of the PHM performances at larger values of λ rather than at λ close to 0. Intuitively, when the component is far from its end of life, the worst decision the PHM system can lead to is the removal of the component from operation. This decision negatively impacts on the component availability, but not on its reliability. On the contrary, when the component approaches its failure time, the decisions based on wrong RUL estimations can lead the component to failure. For this, we can use the value of the stop probability $L = P_\lambda^\alpha + (1 - P_\lambda^\alpha) \times (1 - FN_\lambda)$ in the time region in proximity of failure (i.e., $\lambda \geq 0.75$) as an indicator of the quality level of the PHM system. The value $\lambda = 0.75$ is arbitrarily chosen, as the quality level is introduced only for reducing the number of decision variables to simplify the allocation problem to be tackled. In a real industrial case, other values of λ in the interval $[0.5, 0.9]$ can be used to define the quality level of the PHM system, based on a proper adjustment that responds to the specific characteristics of the application.

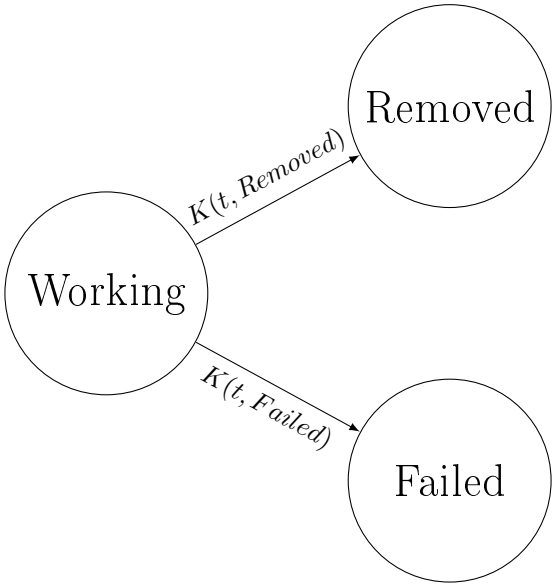

Figure 1: Three-state system

3 Network Reliability Metrics

In this Section, we briefly introduce the network reliability metrics presented in [2] and [3], which will be used to measure the effect on the overall network reliability of the improvements in the reliability of the network elements, due to the PHM system. Notice that relying on these metrics is not mandatory for the application of the proposed PHM-based approach: any metric linking the network failure behavior to the reliability of its constituent parts can be considered.

A topological representation of a generic network can be obtained in terms of the undirected graph $G(V, E)$ [30], where $V = \{1, 2, ..., N_V\}$ is the set of nodes, whereas E is the set of $|E|$ edges connecting the nodes. To simplify the notation, we also consider the set of indexes $E' = \{1, \ldots, |E|\}$, univocally associated to the arcs of E. To establish this relationship, we can, for example, use the relation order "$\prec$", which is defined as: $(i_1, j_1) \prec (i_2, j_2) \iff i_1 < i_2 \vee (i_1 = i_2 \wedge j_1 < j_2)$.

A sequence of nodes $(i_1, i_2, ..., i_k)$, $k > 1$ such that $(i_j, i_{j+1}) \in E,\ 1 \leq j \leq k-1$ forms a path between i_1 and i_k. The set of all paths connecting i to j is $\Gamma_{i,j}$.

Without loss of generality, we focus on the reliability of the network connections only (i.e., we disregards the network nodes). Let $u_{m,n}(t)$ be the unreliability of the edge $(m, n) \in E$ between the pair of nodes m and n at time t and $q_{m,n}(t) = 1 - u_{m,n}(t)$ its the reliability (i.e. the probability of being in state *Working* or *Removed*). Then, the reciprocal of the reliability of the most reliable

path between nodes i and j can be computed $\forall i, j \in V$ as [31]:

$$rd_{i,j}(t) = \min_{\gamma_{i,j} \in \Gamma_{i,j}} \frac{1}{\prod\limits_{(m,n)\in\gamma_{i,j}} (1 - u_{m,n}(t))} = \min_{\gamma_{i,j} \in \Gamma_{i,j}} \frac{1}{\prod\limits_{(m,n)\in\gamma_{i,j}} q_{m,n}(t)} \tag{3}$$

where the minimization is done with respect to all paths $\gamma_{i,j} \in \Gamma_{i,j}$ linking nodes i and j, whereas the product extends to all the edges of each of these paths. Note that $1 \leq rd_{i,j}(t) \leq \infty$, where the lower bound corresponds to the existence of a perfectly reliable path connecting i and j (i.e., $u_{m,n}(t) = 0$, $\forall (m,n) \in \gamma_{i,j}$), whereas ∞ corresponds to the edges i and j being disconnected ($\Gamma_{i,j} = \emptyset$, i.e., it is impossibile to reach node i from node j through the edges belonging to E).
If we take the logarithm in Equation 3, then the minimization problem reduces to a classic shortest path problem ([32], [33], [34]) in a graph, with weights given by $-\log(1 - u_{m,n}(t))$. This allows to exploit well-known algorithms to solve the optimization problem in Equation 3, (e.g., [35]).
Notice also that if edge $(m,n) \in E$ is equipped with a PHM system, then we can use the model developed in [20] to estimate its unreliability $u_{m,n}(t)$ at time t (or, equivalently, its reliability $q_{m,n}(t) = 1 - u_{m,n}(t)$) and, thus, we can estimate rd_{ij} $\forall i, j \in V$.
On this basis, we consider two network reliability metrics, which allow to encode the effect of PHM on the overall network reliability:

1. The global reliability efficiency $E^r[G](t)$ ([2], [3]) of the network G at time t is defined as:

$$E^r[G](t) = \frac{1}{N_V(N_V - 1)} \sum_{i,j=1:N_V; i\neq j} \epsilon^r_{i,j}(t) = \frac{2}{N_V(N_V - 1)} \sum_{i=1:N_V; j>i} \epsilon^r_{i,j}(t) \tag{4}$$

   where $\epsilon^r_{i,j}(t) = \frac{1}{rd_{i,j}(t)} = \frac{1}{rd_{j,i}(t)} = \epsilon^r_{j,i}(t)$ is the most reliable path between i and j and the same as the most reliable path between j and i.

2. The reliability closeness centrality of node i at time t, $RC^C_i(t)$ measures the extent to which a node is near to all other nodes along the most reliable paths:

$$RC^C_i(t) = \frac{N_V - 1}{\sum\limits_{j\in V: j\neq i} rd_{i,j}(t)} \tag{5}$$

   RC^C_i assumes values in the interval $[0, 1]$.

4 PDA setting for optimal allocation of PHM capabilities on the network elements

The final objective of our methodology is the identification of the optimal portfolios (i.e., sets) of actions (i.e., the installation of PHM systems at the network edges E) that maximize the reliability metric $E^r[G](t)$ of a given network $G(V, E)$, provided that these actions are not over-budget.
To formalize this PDA problem, we consider the set of alternative actions $\mathcal{A} = \{L_1, L_2, \ldots, L_\Omega\}$ available at every edge $e = 1, ..., |E|$, representing the PHM systems of different quality levels.
Certainly, the PHM system cost depends on its quality level L; however, to the authors' best knowledge there is yet no robust way to relate the values of the performance metrics of the PHM system to its development cost. In this respect, a first interesting attempt to build such cost model is proposed in [15; 16]. However, this model is not applicable to our setting. Generally speaking, the development of a cost model for PHM is a very challenging task, but out of the scope of this work. Thus, here we apply the SWING ([36]) trade-off weighting approach to give rough cost estimations. Namely, we assume that each action $a \in \mathcal{A}$ entails a cost $C_a \in [10, 100]$ in arbitrary units, such that $L_{a_1} > L_{a_2} \implies C_{a_1} > C_{a_2}$. Then, the best action is assigned cost 100, whereas the worst is assigned cost 10. The cost of the remaining alternatives are roughly estimated by apprising their proximity to these two extreme situations (see [36], [37] and [38] for further details). Notice that the life cycle cost of the PHM system is a fundamental driver for selecting its performance: underestimation of RUL entails unnecessary maintenance costs and the early stoppage of the engineered system. On the contrary, overestimation of RUL can yield to system failure and its associated corrective maintenance cost. The life cycle costs can be much higher than the PHM investment costs, and they heavily depend on the PHM capabilities. Nonetheless, in this work we are concerned with reliability, rather than availability: our goal is to optimize the performance of the network in terms of avoided failures, rather than in terms of increment of the expected portion of time in which the system is working, which the life cycle costs heavily depend on. Further research work dealing with availability optimization will inevitably consider also maintenance costs.
The decision on the action to be applied at the $e-th$ edge, $e = 1, \ldots, |E|$ is indicated by the binary decision variable z_a^e, which is set to 1 if action $a \in \mathcal{A}$ is taken and to 0, otherwise. This way, a portfolio of actions $A \subseteq \mathsf{X}_{e \in E'} \mathcal{A}$ is uniquely defined by the binary vectors $\mathbf{z}^e = [z_a^e]$, $\forall a \in \mathcal{A}$, where $\mathsf{X}_{e \in E'}$ indicates the Cartesian product of the $|E|$ sets $\mathcal{A}$. Obviously, vector $\mathbf{z}^e = [0, ..., 0]$ corresponds to the decision of not taking actions at the $e-th$ edge, $e = 1, ..., |E|$.
We also define the binary vector $\mathbf{z}$ as the concatenation of vectors $\mathbf{z}^e$, $\forall e \in E'$, whose $k-th$ element reads:

$$z_k = z_{1+(k-1) \bmod \Omega}^{e=\lfloor \frac{k}{\Omega} \rfloor + 1}, \; k = 1, \ldots, |E| \times \Omega. \tag{6}$$

This way, the relation between $\mathbf{z}$ and the portfolio $\mathcal{A}$ is bijective.
The optimization problem at time t can be formulated as:

$$\max_{\mathbf{z}} E^r[G](t) \tag{7}$$

subject to the constraints

$$\sum_{a\in\mathcal{A}, e\in E'} z_a^e C_a \leq B \tag{8}$$

$$\sum_{a\in\mathcal{A}} z_a^e \leq 1 \qquad \forall e \in E' \tag{9}$$

$$z_a^e \in \{0,1\} \qquad \forall e \in E', \forall a \in \mathcal{A} \tag{10}$$

Equation 8 formalizes that the portfolio cost must be smaller than the available budget B, whereas Equations 9-10 state that at most one action can be pursued at each edge, $e = 1, \ldots, |E|$.
Notice that the optimization problem we are dealing with requires to compute $E^r[G](t)$ for every feasible portfolio (i.e., every portfolio respectful of the constraints), which, in its turn, requires to solve the minimization problem in Equation 3 for all the $\frac{N_V(N_V-1)}{2}$ pairs of nodes (see Equation 4). From these considerations, it clearly emerges that on one side, the computational burden to address the optimization problem rapidly increases as the number of edges and number of actions at each edge increase. On the other side, the objective function in Equation 7 is strongly non-linear; this prevents us from using the integer linear programming algorithms developed by Liesiö et al., within the Robust Portfolio Modeling framework to find the exact solution to the optimization problem ([39], [40]).
To solve the optimization problem, then, we use the Genetic Algorithms (GA, e.g., [41]), which are stochastic search meta-heuristics, belonging to the larger class of the evolutionary algorithms: they mimic the process of natural evolution, such as inheritance, mutation, selection and crossover, to extract the fittest individuals with respect to the objective function.

5 Case Study

The optimization framework illustrated above is applied to the transmission network system IEEE 14 BUS [23], which has been taken as reference case study in several works of the literature (e.g., [42], [43]).
The IEEE 14 BUS system is a portion of the American Electric Power System consisting of 14 bus locations connected by 20 lines and transformers (Figure 2). The transmission lines operate at two different voltage levels, 132 kV and 230 kV, with three 230/132 kV tie stations (Buses 4, 5 and 7)

and two generating units (Buses 1 and 2). The network is also provided with voltage corrective devices (i.e., synchronous condensers) in correspondence of Buses 3, 6 and 8.

According to [2] and [3], every network edge is supposed to have a failure behavior obeying an exponential distribution, whereby the unreliability of edge $(m,n) \in E$ at time horizon T is $u_{m,n}(T) \sim \mathcal{E}(\lambda_{m,n}) = 1 - e^{-\lambda_{m,n}T}$. Notice that the equivalent time λ is different from the edges failure rate, $\lambda_{m,n}$ (i.e., with subscript), although we indicate them with the same letter; we do this because of the common use of this letter in the respective fields.

The failure rate values of the IEEE 14 BUS network are reported in Figure 3, which shows the graph model of the IEEE 14 BUS network. These values, which are derived from [30], mainly depend on the type of line (transmission or transformer) and its voltage value. Yet, in Figure 3 we can also note that the failure rates of the edges located in the central part of the network are 50 times smaller than those of the edges in the left part of the network and 100 times smaller than those of the edges in the right part.

Notice that although the reliability of the edges is assumed to obey the exponential distribution, this choice is not mandatory for the applicability of the proposed framework, whereby any probability distribution can be used. In particular, components of power transmission networks reliability are affected both by ageing failures and shock failures, and the reliability model should encode both these two competing mechanisms [44]. This extension will be considered in future research work.

In Figure 3, every node is assigned a triplet of numbers: the first represents the node identification number $i = 1, \ldots, 14$, whereas the second and the third numbers represent the ranking positions of the node with respect to the $RC^C(T)$ values at $T = 1$ and $T = 10$, respectively, sorted in descending order (i.e., rank 1 corresponds to the largest $RC^C(T)$ value and rank 14 to the smallest one).

The ranking of the nodes is not very sensitive to the time horizon duration, as only two nodes (i.e., 2 and 8) experience significant changes in the ranking positions. However, just these changes, which need a numerical analysis for their justification, tell us that different horizons entail different decision problems. For this, we show the results of the optimization for $T = 1$ and $T = 10$, which correspond to short-term and long-term decision-making problems, respectively.

To estimate through Equation 2 the reliability improvement brought by the PHM capability, we consider the following numerical setting. With respect to maintenance policy data, we set $h = 3$, $\alpha = 0.1$, $\Delta t = 0.05$ and $\beta = 90$.

With respect to the PHM metrics, we assume that DTD follows a log-normal distribution with mean 0.1 and standard deviation 0.0001. FP_λ is a step-wise function such that $FP_\lambda = 0.1,\ \lambda \in [0, 0.75)$ and $FP_\lambda = 0.2,\ \lambda \in [0.75, 1]$, $FN_\lambda = 1 - FP_\lambda$ and P_λ^α is a step-wise increasing function over the $\lambda-$intervals $[0, 0.25)$, $[0.25, 0.5)$, $[0.5, 0.75)$, $[0.75, 1]$.

Notice that these values are illustrative; for a real application, a procedure for their estimation must be implemented, which has been proposed in [20].
Notice also that FP_λ and FN_λ can strongly depend on λ. Nonetheless, since we want to solve the allocation problem with a limited number of decision variables, we consider the performance metric values only in the last region of Figure 16. These are set so that we have three PHM systems with sensibly different performance levels L. This allows clearly assessing the impact of PHM on the global network reliability. Further research work dealing with real network systems and PHM prognostic algorithms will consider the complete behavior of the prognostics performance metrics. The sensitivity of the network edge reliability to the values of FP_λ and FN_λ is analyzed in Appendix C.

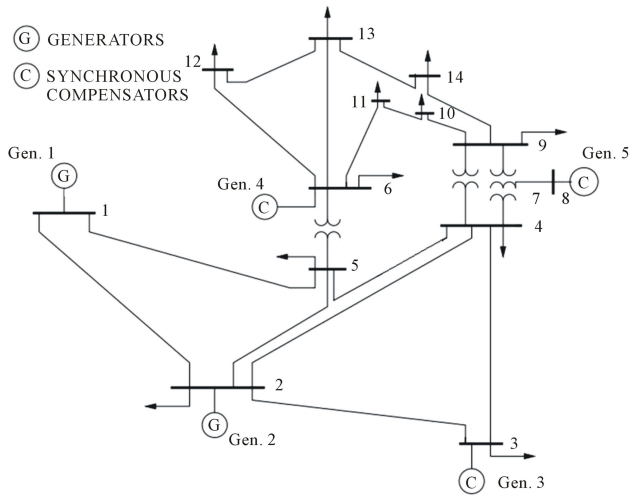

Figure 2: IEEE 14 network physical lines

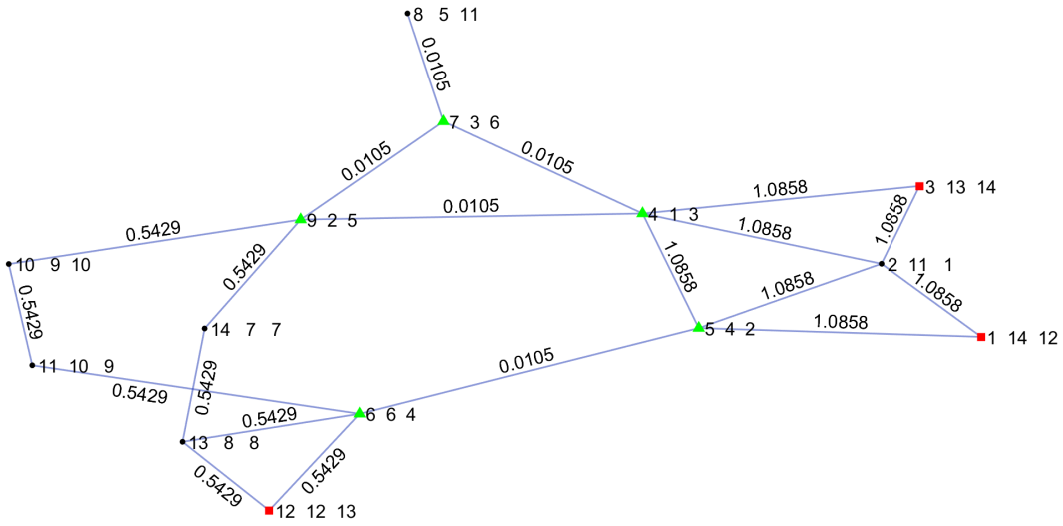

Figure 3: IEEE 14 network graph representation. The 5 most important nodes with respect to both time horizons (i.e., 4, 5, 6, 7, 9) are indicated with marker $\triangle$, whereas the 3 least important (1, 3, 12) with marker $\square$.

The selected performance values entail that the PHM quality level indicator L assumes three possible values $L_1 = 0.28$, $L_2 = 0.6$ and $L_3 = 0.8$, which is summarized in Table 1 and corresponds to development costs $C_1 = 10$, $C_2 = 70$ and $C_3 = 100$ in arbitrary units, respectively. Notice that this quality level indicator L can be the result of many other different combinations of metric values .

Finally, to apply Equation 2 we need to know the distributions of T_d and T_ϕ, provided that T_f obeys the exponential law with rate $\lambda_{m,n}$ ([2], [3]). To this aim, we can assume that T_d and T_ϕ obey gamma distributions to exploit the well-known properties ([45]):

- Given $T_d \sim \mathcal{G}(\alpha_{\mathcal{G}_1}, \lambda_{m,n})$ and $T_\phi \sim \mathcal{G}(\alpha_{\mathcal{G}_2}, \lambda_{m,n})$, then $T_f = T_d + T_\phi \sim \mathcal{G}(\alpha_{\mathcal{G}_1} + \alpha_{\mathcal{G}_2}, \lambda_{m,n})$
- $T_f \sim \mathcal{G}(1, \lambda_{m,n})$ is equivalent to $T_f \sim \mathcal{E}(\lambda_{m,n})$.

λ interval \ a	L_1	L_2	L_3
[0.0.25)	0.28	0.28	0.28
$[0.25, 0.5)$	0.28	0.39	0.46
$[0.5, 0.75)$	0.28	0.5	0.62
$[0.75, 1]$	0.28	0.6	0.8

Table 1: Performance level indicator L in different $\lambda-$intervals

On this basis, we can express the mean time to reach the detection threshold $\mathbb{E}[T_d] = \frac{\alpha_{\mathcal{G}_1}}{\lambda_{m,n}}$ as a portion χ of the the mean time to reach the second threshold $\mathbb{E}[T_\phi] = \frac{\alpha_{\mathcal{G}_2}}{\lambda_{m,n}}$, i.e., $\mathbb{E}[T_d] = \chi\mathbb{E}[T_\phi]$, and impose $\alpha_{\mathcal{G}_1} + \alpha_{\mathcal{G}_2} = 1$, to get $T_f \sim \mathcal{G}(1, \lambda_{m,n})$. For example, we set $\chi = \frac{1}{3}$, which entails that $\frac{\alpha_{\mathcal{G}_1}}{\lambda_{m,n}} = \frac{1}{3}\frac{\alpha_{\mathcal{G}_2}}{\lambda_{m,n}}$ and $\frac{1}{3}\alpha_{\mathcal{G}_2} + \alpha_{\mathcal{G}_2} = 1$; then, $\alpha_{\mathcal{G}_1} = \frac{1}{4}$ and $\alpha_{\mathcal{G}_2} = \frac{3}{4}$.

6 Results and discussion

6.1 Optimization results

To evaluate the impact of the budget on the optimal action portfolio, we solve the optimization issue for different budget levels: for this, B is taken in $[20, 600]$ (i.e., from 2 times the minimum cost of a PHM system, up to 6 times its maximum cost) at discrete values equally spaced by 20, in arbitrary units.

The GA settings are summarized in Table 2. The population size value trades off the need of having genetic diversity among the population chromosomes, against the need of avoiding excessive population size, which entails computational burdens. Similar reasoning guided us towards the choice of the crossover probability and the selection rule. The number of maximum generations has been conservatively set to 1000, based on the observation that the population contains many similar chromosomes after $150-200$ iterations of the algorithm, in correspondence of a constant maximum value of the reliability index. Finally, the penalty value on constraint violation has been set equal to the maximum cost of a PHM system (i.e., 100), which prevents from achieving unfeasible solutions.

Population Size	200
Max Stall Generations	50
Max Generations	1000
Selection	Fit-Fit
Replacement	Children-Parents
Crossover probability	0.8
Constraint Penalty	100

Table 2: GA parameters settings

To speed up the computation, before launching the GA we have estimated through Equation 2 the edge reliability values at $T = 1$ and $T = 10$ of all the possible combinations of the three failure rate values (i.e., $\lambda_{m,n} = 0.0105, 0.5429, 1.0858$) and the $\Omega = 3$ actions $\mathcal{A} = \{L_1, L_2, L_3\}$. The results, obtained by applying the Monte Carlo procedure described in [20] are summarized in Tables 3 and 4.

From the analysis of these Tables, we can notice that at least one third of the edges, whichever their failure rate values, are expected to be *Working* or *Removed* at $T = 1$, whereas almost all the edges are expected to be *Failed* at $T = 10$ if no action $a \in \mathcal{A}$ is pursued.

Due to the small values of the failure rates of the edges in the central part of the network, these have very large reliability values (i.e., $q_{m,n} \geq 0.98$ at $T = 1$ and $q_{m,n} \geq 0.9$ at $T = 10$) even when no action is taken.

The benefit of PHM is more appreciable on edges with large failure rates. In fact, from both Tables 3 and 4 we can see that the reliability of the components with failure rate $\lambda = 0.0105$ does not increase more than 10% even if the best PHM system is installed (first rows in Tables 3-4), whereas in case of $\lambda = 1.0858$, $a = L_3$ yields an increment in reliability of more than 100% with respect to $a = \emptyset$ (Tables 3-4, third row).

Finally, for every failure rate value, the largest reliability improvement is gained switching from $a = \emptyset$ to $a = L_1$, whereas the benefit of $a = L_3$ is more appreciable when $T = 10$: the edges equipped with the best PHM system have the smallest drop in reliability, switching from $T = 1$ to $T = 10$.

$\lambda_{m,n}$ \ a	$\emptyset$	L_1	L_2	L_3
0.0105	0.9896	0.9940	0.9958	0.9961
0.5429	0.5811	0.7495	0.8085	0.8267
1.0858	0.3376	0.5883	0.6726	0.6974

Table 3: Reliability values $q_{m,n}$ of the edges corresponding to $a \in \mathcal{A}$, $T = 1$

$\lambda_{m,n}$ \ a	$\emptyset$	L_1	L_2	L_3
0.0105	0.9003	0.9555	0.9824	0.9900
0.5429	0.0044	0.4924	0.7145	0.7748
1.0858	0.0000	0.4363	0.6137	0.6636

Table 4: Reliability values $q_{m,n}$ of the edges corresponding to $a \in \mathcal{A}$, $T = 10$

As usual in PDA ([39; 40]), we evaluate the behavior of $E^r[G](T = 1, 10)$ versus different budget levels B (Figure 4). Both curves have an elbow point (at $B = 120$ and at $B = 100$ for $T = 1$ and $T = 10$, respectively), where there is an abrupt change in the slope of the curve causing the reliability efficiency metric to grow more slowly: any increase in B after the elbow does not provide improvements as valuable as before the elbow point. Then, the elbow points represent the best investment in case the budget is limited although with no specific indication about its maximum and there is no constraint on $E^r[G](T = 1, 10)$ [39], [40].

The curve corresponding to $T = 1$ is always above that corresponding to $T = 10$, even if their gap decreases as the budget increases: as mentioned above, the larger the budget, the larger the number of actions $a = L_3$ taken on the edges, which reduce the difference between the reliability values of the network elements at $T = 1$ and $T = 10$ (Tables 3-4, last column).

Notice that the $E^r[G]$ values are not monotonously increasing with the increasing budget levels (e.g., at $B = 350$ for $T = 10$ years). This is due to GA, which is not always capable of finding the global optimum: especially for large budgets, there are many portfolios with very similar reliability efficiency values, which lead the GA to be trapped in local maxima.

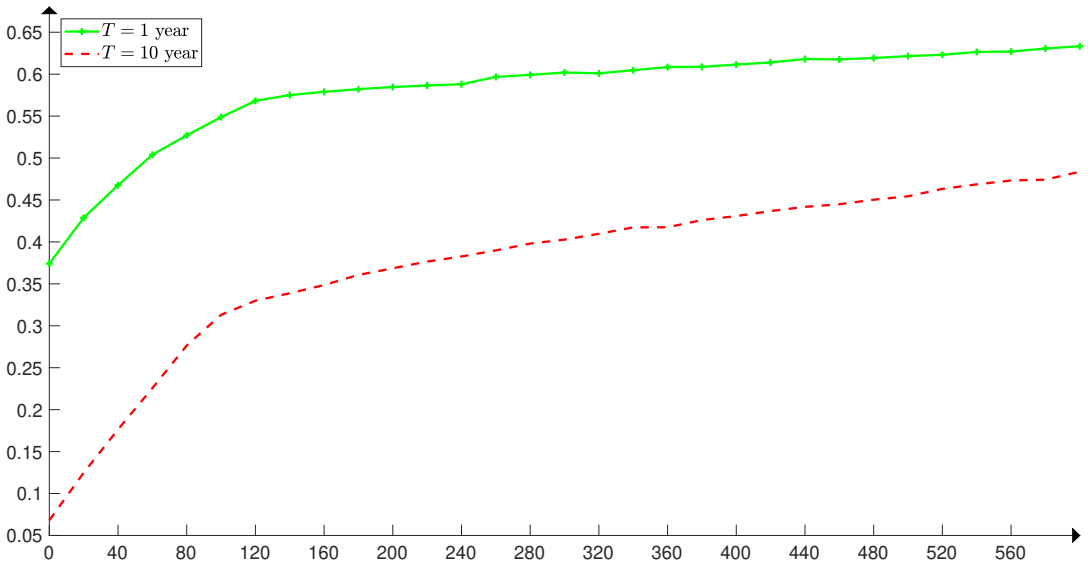

Figure 4: $E^r[G]$ vs budget level

Figures 5a and 5b show the number of actions $a \in \mathcal{A}$ on the network vs budget level. From these Figures, we can notice that the best solutions favor the investment in large numbers of cheap actions rather than in small numbers of expensive actions. Yet, in correspondence to larger budget levels, the number of actions $a = L_3$ at $T = 10$ is larger than that at $T = 1$. This is due to the more appreciable reliability improvement brought by $a = L_3$ at larger time horizons (see Tables 3 and 4).

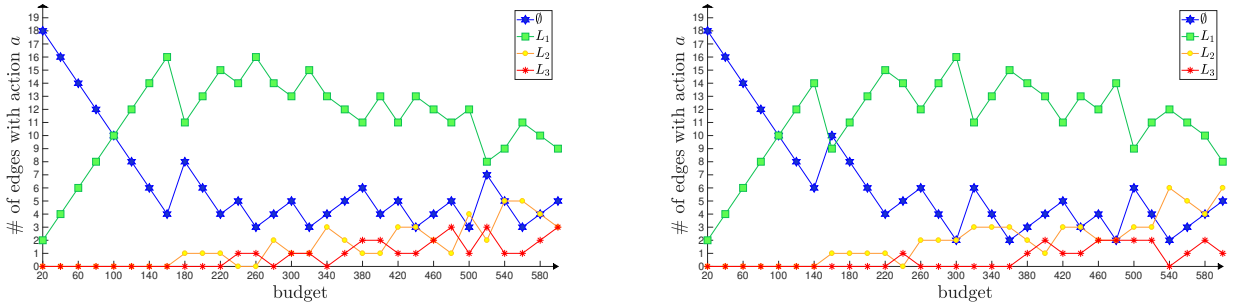

(a) $T = 1$ (b) $T = 10$

Figure 5: Number of actions a vs budget level for different time horizons

Figures 6-10 show in details the optimal portfolios found by GA at the different budget levels.

For both time horizons $T = 1, T = 10$, edge $(4, 5)$ is the first edge where actions are taken and it is also the edge where action $a = L_3$ is taken for the first time. This is due to the fact that edge $(4, 5)$ is the only edge with the largest failure rate $\lambda_{4,5} = 1.0858$ connecting two of the most reliability-central nodes. The other edge selected at $B = 20$ is $(3, 4)$ when $T = 1$ and $(9, 10)$ when $T = 10$. This difference confirms that the optimal solutions generally depend on the time horizon we are referring to.

At $T = 1$, the edges with failure rate 0.0105 are hardly ever chosen as optimal locations for actions, whereas at $T = 10$ there is a larger presence of these edges in the optimal action portfolios. This is also due to the fact that at $T = 10$ the differences among the values of intrinsic reliability and PHM reliability are larger than those at $T = 1$, which makes convenient investing in higher PHM quality levels.

The behavior at $T = 10$ is characterized by many more fluctuations of portfolios, due to the similarity of the portfolios selected in the final population of the GA.

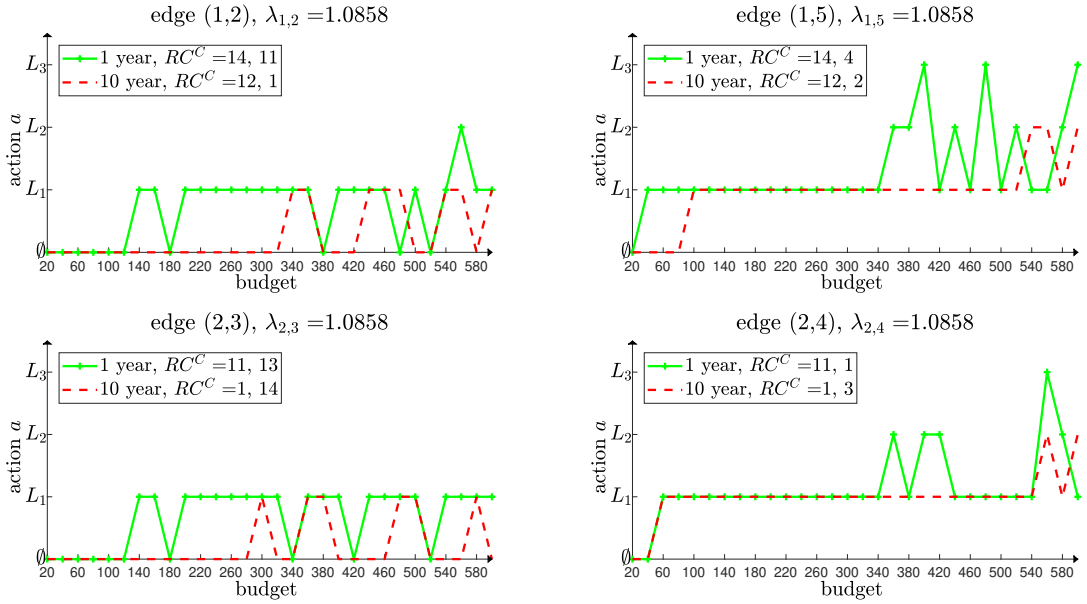

Figure 6: Action a vs budget for edges 1-4

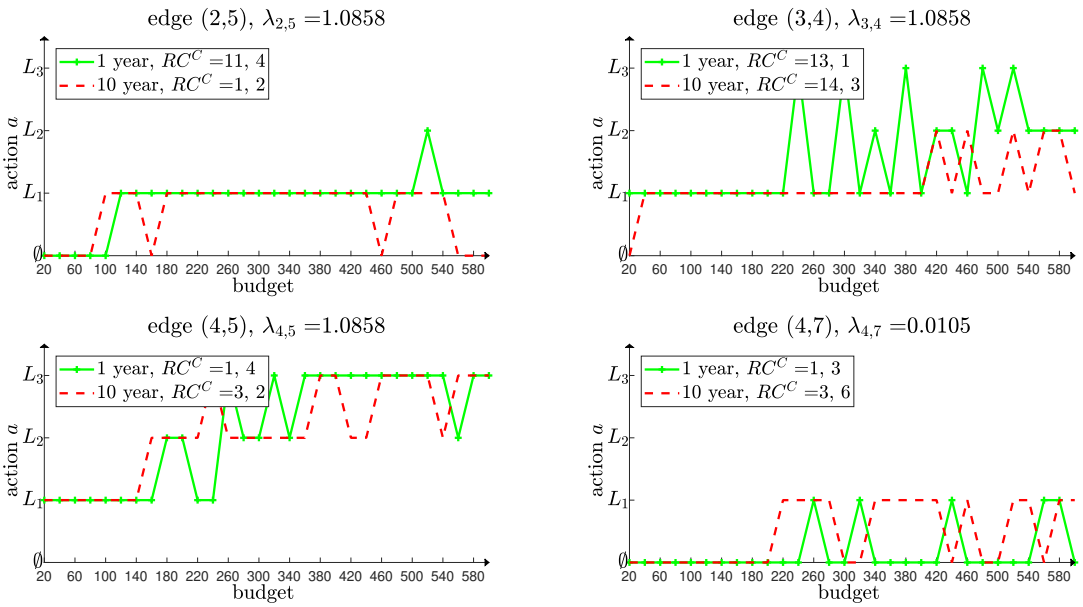

Figure 7: Action a vs budget for edges 5-8

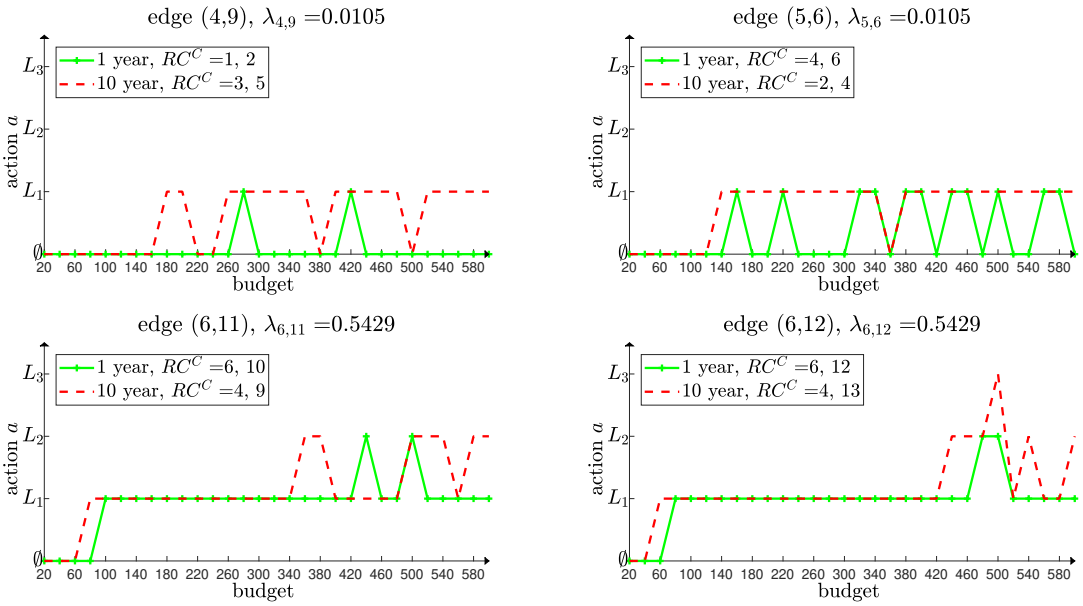

Figure 8: Action a vs budget for edges 9-12

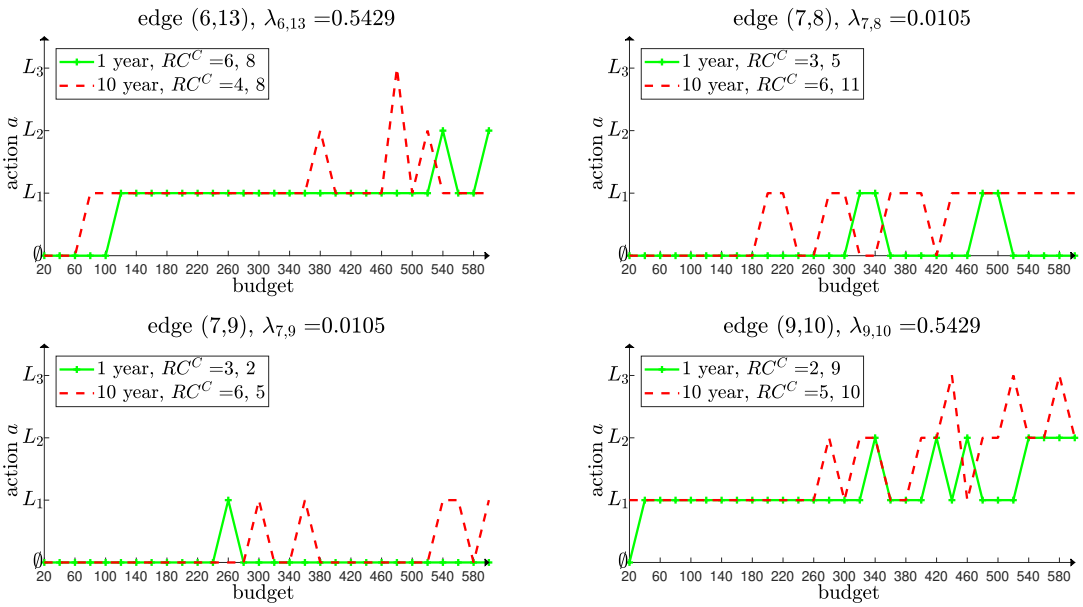

Figure 9: Action a vs budget for edges 13-16

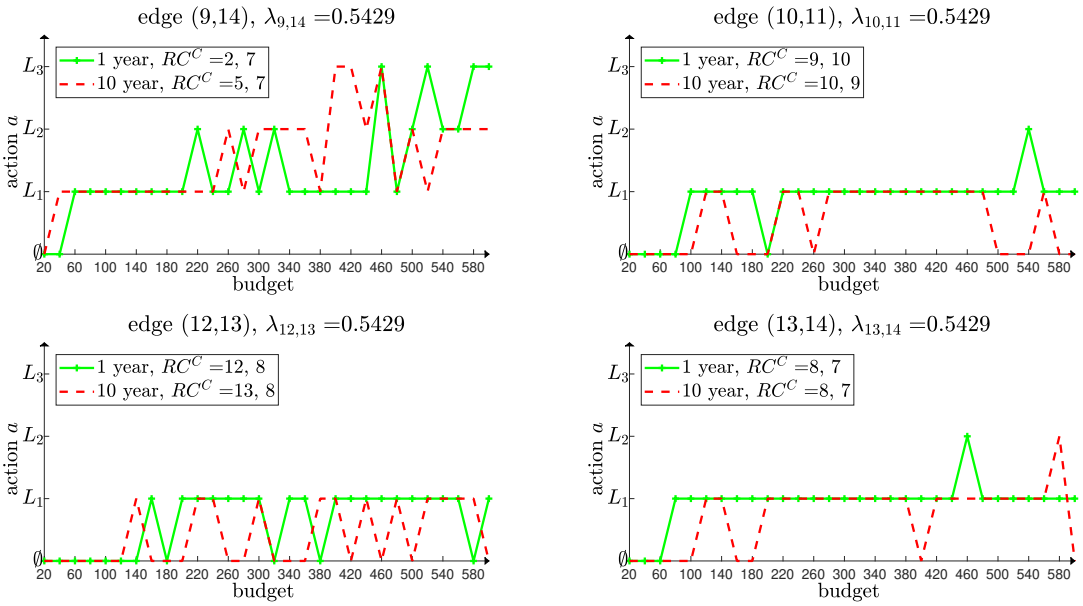

Figure 10: Action a vs budget for edges 17-20

Figure 11 shows an example of optimal portfolios for four different budget levels $B = 100, 260, 420, 580$, at $T = 1$. The values on the edges in Figure 11 indicate their reliability values multiplied

by 1000, whereas the triplet of values on the nodes indicate their identification number, their $RC^C(T = 1)$ rank in the initial configuration and their rank in the optimal action portfolio configuration. From the analysis of the Figure, we can see that actions are rarely taken on the edges of the central part of the network.
With respect to the ranking of the RC^C values, although this is impacted from the actions taken on the nodes (the ranks of some nodes change in the optimal configuration), however the rank differences are not very large and actions are taken in a sort of balanced allocation between the right and the left part of the network.

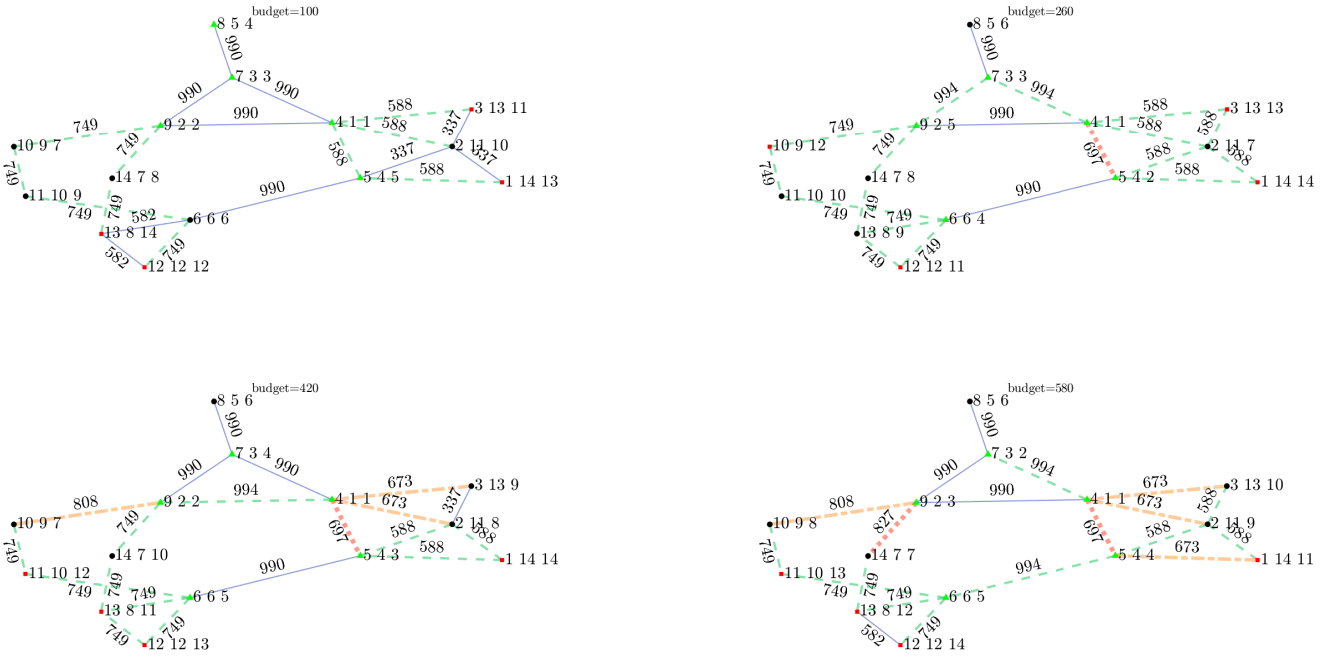

Figure 11: Network graphs corresponding to the optimal solutions at budget levels $100, 260, 420, 580$, $T = 1$. Edges where $a = \emptyset$ are indicated by continuous lines, those with $a = L_1$ by dashed lines, $a = L_2$ by dashed-dotted lines and $a = L_3$ by dotted lines.

The same reasoning applies to Figure 12, which represents the same information as in Figure 11, but referred to $T = 10$. However, in this case, we can notice that actions $a = L_1$ are taken also on the edges of the central part of the network, because there is a more appreciable increase in the reliability when switching from the situation of $a = \emptyset$ to $a = L_1$ at $T = 10$ (Tables 3 and 4).
We can see also a general increase in the number of actions $a = L_2$.

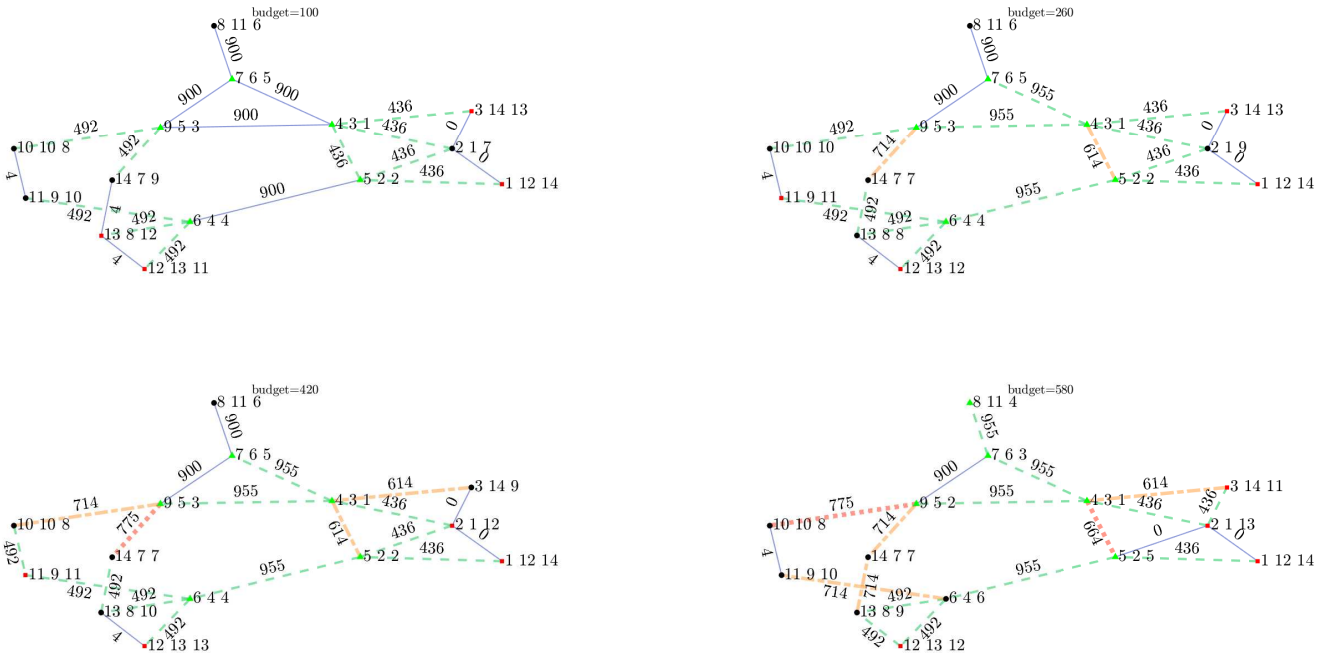

Figure 12: Network graphs corresponding to the optimal solutions at budget levels $100, 260, 420, 580$, $T = 10$. Edges where $a = \emptyset$ are indicated by continuos lines, those with $a = L_1$ by dashed lines, $a = L_2$ by dashed-dotted lines and $a = L_3$ by dotted lines.

6.2 Comparison between portfolio optimization and intuitive approaches

To highlight the relevance of the proposed optimization approach, we consider some alternative intuitive approaches for decisions making to compare their results. For simplicity, we consider that only the cheapest action $a = L_1$ is available; this is due to the fact that the elbow point of the decision task is located at $B = 100/120$, whereby choosing the best portfolio of solutions is particularly important when the budget is very limited. For this, we assume that B ranges in $[20, 100]$ with discrete values equally spaced by 20.
The alternative intuitive methods are:

1. "Most central first". This approach consists in an iterative procedure such that the most important node (i.e., with largest $RC_i^C(t)$) with at least one connected edge not equipped with PHM is identified and actions are applied to reduce its failure probability. Then, $RC_i^C(t)$ are calculated again to determine the most important node in the improved system, whereafter further actions are pursued to increase the network reliability $E^r[G](t)$. This procedure is repeated until the budget is depleted. This approach is derived from [25], with the difference that in our framework the centrality measure indicates the most reliable component instead

of the least reliable one. Notice that, if there is more than one edge insisting on the most important node, then we randomly select one out of them to apply $a \in \mathcal{A}$.

2. "Least central first". In this case, we apply the same iterative procedure as before but working first on the least central node. Namely, RC_i^C is computed $\forall i \in V$ and the nodes are sorted in descending order based on this value. Using this ranking, the first node i' is chosen such that at least one edge surrounding it is not equipped with PHM. Then, actions are taken on the least reliable edge among those insisting on i'. If there are multiple edges with same failure rate value, we randomly choose one among them. The procedure is repeated as long as the budget is finished.

3. "Failure rate". If we sort the reliability values of the edges in E in the set $\mathcal{Q} = \{q_1, q_2, \ldots, q_Q\}$, with $|\mathcal{Q}| = Q \leq |E|$, $0 \leq q_i \leq 1 \; \forall i \leq Q$, $q_i < q_{i+1}$, the first edge is chosen randomly among those with reliability q_1. Then the procedure is repeated as long as the edges with reliability q_1 are all equipped with PHM. Then, the edges with reliability q_2 are considered and the same approach as before is followed. The procedure is iterated as long as the budget of the portfolio optimization is finished.

4. "Hybrid" From the analysis of the optimization results (Section 6), which show that the edges with failure rate 0.0105 are hardly ever chosen as an optimal location to set PHM, we propose a slightly different version of the approaches above. The rule is simple: follow the steps of approach "Most central first" but do not take actions on edges whose failure rate is 0.0105. This approach is an hybrid solution between "Failure rate" and "Most central first".

We present the results of the comparison between PDA and the intuitive approaches for time horizons $T = 1, 2, 5, 10$. Notice that, in principle, the value of $E^r[G](t)$ obtained by following the intuitive approaches is stochastic, because all these methods require a random selection among edges. For this reason, for each of these approaches and for every different budget level, we run $H = 10000$ Monte Carlo simulations to compute the expected value of $E^r[G](t)$.
Figure 13 shows $\mathbb{E}[E^r[G](t)]$ versus budget B and time horizon T. From the analysis of this Figure, we can notice that the results obtained from the Portfolio Optimization are always above those of the other approaches, especially for larger time horizons. The worst approach is "Least central first"; this suggests that the edges around nodes which are not reliability-central are not effective, no matter how poor their reliability charateristics are.
The approach "Most central first" tends to install PHM systems on the edges insisting on the nodes with the highest RC^C values, thus causing the level of these nodes to increase more and more. In turn, PHM system is always installed on the nodes in the middle of the network, which have the higher degree, and, thus, PHM is selected also on nodes with failure rate 0.0105, which

is not an effective action. This drawback is circumvented by the "Hybrid" approach, which turns out to be the best one (i.e., closest to PDA).

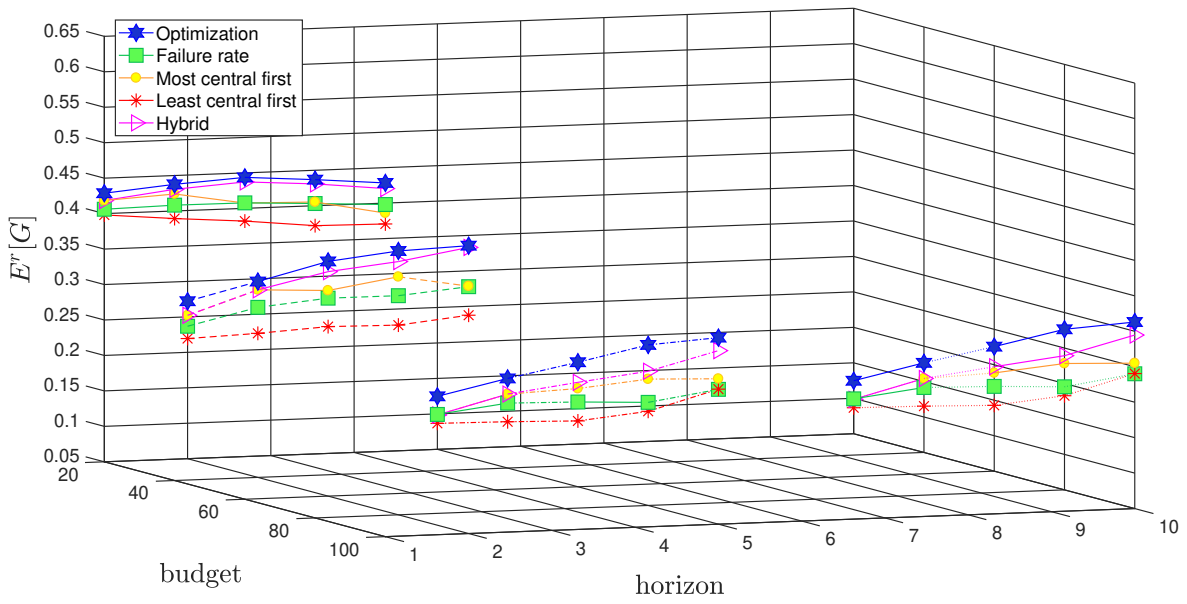

Figure 13: Comparison of PDA with intuitive approaches

In details, Figure 14, highlights the differences between the "Most central first" and "Hybrid" approaches. The first number on each edge indicates the probability that PHM is set on that node under "Most central first" approach, wheras the second indicates the probability that PHM is set on that node under "Hybrid" approach. Notice that for budget $B \leq 40$ the results are the same; little discrepancies are mainly due to Monte Carlo simulation. On the contrary, when the available budget increases, then the "Most central first" method tends to allocate actions on the edges of the central part of the network. For example, "Hybrid" approach never takes actions on edge $(4, 9)$, which connects two among the most important nodes. On the contrary, the "Most central first" approach tends to select this edge just because it insists on the central node $i = 4$.

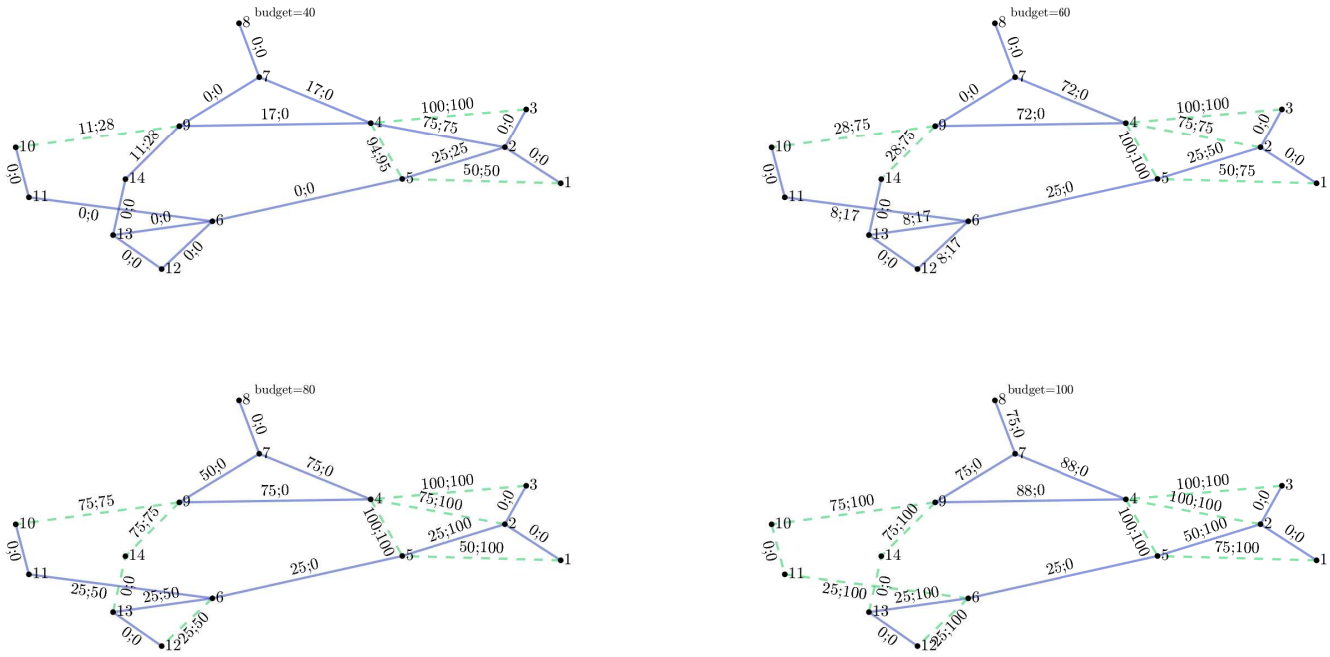

Figure 14: Comparison between "Most central first" and "Hybrid"

7 Conclusion

In this work we have proposed a novel framework to quantify the increase in reliability of a power transmission network when its elements are provided with PHM capabilities. The method relies on the one hand on an analytic, time-variant model, which conservatively evaluates the increase in reliability achievable when a network element is equipped with a PHM system of known performance metrics. On the other hand, it relies on a global reliability index of the network (i.e., the global reliability efficiency) which establishes a link between the reliability improvement at the network elements with the global reliability behavior. On this basis, we have exploited methods of Portfolio Decision Analysis (PDA) to find the portfolios of PHM systems to be installed on a network which maximize the network global reliability efficiency under the given budget constraints. To highlight the worth of addressing the PHM-based network reliability optimization within PDA, we have compared the optimal solutions with those of alternative intuitive approaches. This comparison has shown that the PDA is the only way to guarantee an optimal investment. Finally, this contribution paves the way to many research issues, which include:

- considering additional optimization criteria such as different network reliability or resilience metrics.

- Using the availability model of PHM-equipped components developed in [20] to consider the transitions back to the working state and evaluating as outage/unavailability the time spent out of that state.
- Developing a framework to link the PHM performance metrics to the PHM development cost.
- Developing an exact algorithm for the solution of the proposed PDA model and/or the generalization of the PDA model (e.g. by means of enhancements Robust Portfolio Modeling (RPM), so as to take into account the uncertainty in PHM metrics values and cost).
- Considering a larger network and handling the related computational issues.

References

[1] P. Hines, S. Blumsack, *A centrality measure for electrical networks*, IEEE, Hawaii International Conference on System Sciences, Proceedings of the 41st Annual (2008).

[2] F. Cadini, E. Zio, C. A. Petrescu, *Optimal expansion of an existing electrical power transmission network by multi-objective genetic algorithms*, Reliability Engineering & System Safety 95.3 (2010): 173-181.

[3] E. Zio, L. R. Golea, *Identifying groups of critical edges in a realistic electrical network by multi-objective genetic algorithms*, Reliability Engineering & System Safety 99 (2012): 172-177.

[4] J. Choi, T. Tran, A. A. El-Keib, R. Thomas, H. Oh, R. Billinton, *A method for transmission system expansion planning considering probabilistic reliability criteria*, IEEE Transactions on Power Systems 20.3 (2005): 1606-1615.

[5] F. Roos, *Electricity Supply Reliability Evaluation of Improvement Solutions for Existing Electricity Networks*, ISBN 91-88934-41-1, Lund (2005).

[6] H. Lågland , *Comparison of different reliability improving investment strategies of Finnish medium-voltage distribution systems* , ISBN 978–952–476–384–4, Acta Wasaensia 256 (2012).

[7] Y.-P. Fang, N. Pedroni, E. Zio, *Comparing network-centric and power flow models for the optimal allocation of link capacities in a cascade-resilient power transmission network*, IEEE Systems Journal, 11.3 (2017): 1632-1643.

[8] E. Zio, R. L. Golea, G. Sansavini, *Optimizing protections against cascades in network systems: A modified binary differential evolution algorithm*, Reliability Engineering & System Safety 103 (2012): 72-83.

[9] N. Yodo, P. Wang., *Resilience allocation for early stage design of complex engineered systems*, Journal of Mechanical Design 138.9 (2016): 091402.

[10] E. Zio, M. Compare, *Evaluating maintenance policies by quantitative modeling and analysis*, Reliability Engineering & System Safety 109 (2013): 53-65.

[11] E. Zio,*Challenges and opportunities in reliability engineering: the big KID (Knowledge, Information and Data)*, IEEE, Transactions on Reliability, 65.4 (2016): 1769 - 1782.

[12] F. Black, R. Litterman, *Global portfolio optimization*, Financial analysts journal 48.5 (1992): 28-43.

[13] X. S. Si, W. Wang, C.H. Hu, D.H. Zhou,*Remaining useful life estimation - A review on the statistical data driven approaches*, European Journal of Operational Research, 213.1 (2011): 1-14.

[14] E. Zio, *Prognostics and health management of industrial equipment*, Diagnostics and Prognostics of Engineering Systems: Methods and Techniques (2012): 333-356.

[15] B. D. Youn, C. Hu, P. Wang, *Resilience-driven system design of complex engineered systems*, Journal of Mechanical Design, 133.10, (2011): 101011.

[16] J.T. Yoon, B.D. Youn, M. Yoo, Y. Kim, *A newly formulated resilience measure that considers false alarms*, Reliability Engineering & System Safety, 167 (2017): 417-427.

[17] A. Saxena, J. Celaya, B. Saha, S. Saha, K. Goebel, *Evaluating algorithm performance metrics tailored for prognostics*, IEEE, Aerospace conference (2009): 1-13.

[18] B. Saha, K. Goebel, *Modeling Li-ion battery capacity depletion in a particle filtering framework*, Proceedings of the annual conference of the prognostics and health management society (2009): 2909-2924.

[19] A. Saxena, K. Goebel, D. Simon, N. Eklund, *Damage propagation modeling for aircraft engine run-to-failure simulation*, IEEE, PHM 2008, International Conference on Prognostics and Health Management (2008): 1-9.

[20] M. Compare, L. Bellani, E. Zio, *Reliability model of a component equipped with PHM capabilities*, Reliability Engineering & System Safety, 168 (2017): 4-11.

[21] A. Salo, J. Keisler and A. Morton (eds.), *Portfolio Decision Analysis: Improved Methods for Resource Allocation*, Springer International Series in Operations Research & Management Science, Vol. 162, Springer, New York (2011).

[22] J. Klapka, P. Piňos, *Decision support system for multicriterial R&D and information systems projects selection*, Eur. J. Oper. Res. 140.2 (2002): 434-446.

[23] The IEEE 14 BUS data can be found on, http://www.ee.washington.edu/research/pstca/.

[24] T. Aven, P. Baraldi, R. Flage, E. Zio, *Uncertainty in Risk Assessment: The Representation and Treatment of Uncertainties by Probabilistic and Non-Probabilistic Methods*, John Wiley & Sons (2014).

[25] M. C. Cheok, G. W. Parry, R. R. Sherry, *Use of importance measures in risk-informed regulatory applications*, Reliability Engineering and System Safety 60 (1998): 213-226.

[26] E. Zio, L. Podofillini, *Importance measures and genetic algorithms for designing a risk-informed optimally balanced system*, Reliability Engineering and System Safety 92.10 (2007): 1435-1447.

[27] A. Mancuso, M. Compare, A. Salo, E. Zio, *Portfolio optimization of safety measures for reducing risks in nuclear systems*, Reliability Engineering and System Safety 167 (2017): 20-29.

[28] E. Zio, *The Monte Carlo Simulation Method for System Reliability and Risk Analysis*, Springer, (2013).

[29] E. Zio, *Computational methods for Reliability and Risk Analysis*, Springer, (2009).

[30] R. Billinton, W. Li, *Reliability Assessment of Electric Power Systems Using Monte Carlo Methods*, Springer (1994): 19-20.

[31] E. Zio, *From complexity science to reliability efficiency: a new way of looking at complex network systems and critical infrastructures*, International Journal of Critical Infrastructures 3.3-4 (2007): 488-508.

[32] E. W. Dijkstra, *A note on two problems in connexion with graphs*, Numerische mathematik 1.1 (1959): 269-271.

[33] D. B. West, *Introduction to graph theory*, Vol. 2. Upper Saddle River: Prentice hall (2001).

[34] M. Desrochers, F. Soumis, *A reoptimization algorithm for the shortest path problem with time windows*, European Journal of Operational Research 35.2 (1988): 242-254.

[35] D. B. Johnson, *Efficient algorithms for shortest paths in sparse networks*, Journal of the ACM 24.1 (1977): 1-13.

[36] D. Von Winterfeldt, W. Edwards, *Decision Analysis and Behavioural Research*, Cambridge University Press, Cambridge (1986).

[37] W. Edwards, *How to use multiattribute utility measurement for social decision making*, IEEE Transactions on Systems, Man and Cybernetics 7 (1977): 326-340.

[38] W. Edwards, F. H. Barron, *SMARTS and SMARTER: Improved simple methods for multiattribute utility measurement*, Organizational Behaviour and Human Decision Processes 60 (1994): 306-325.

[39] J. Liesiö, P. Mild, A. Salo, *Robust portfolio modeling with incomplete cost information and project interdependencies*, European Journal of Operational Research 190.3 (2008): 679-695.

[40] J. Liesiö, P. Mild, A. Salo, *Selecting infrastructure maintenance projects with Robust Portfolio Modeling*, Decision Support Systems 77 (2015): 21-30.

[41] M. Marseguerra, E. Zio, S. Martorell, *Basics of genetic algorithms optimization for RAMS applications*, Reliability Engineering & System Safety 91.9 (2006): 977-991.

[42] S. Ghosh, S. P. Ghoshal, S. Ghosh, *Optimal sizing and placement of distributed generation in a network system*, International Journal of Electrical Power & Energy Systems 32.8 (2010): 849-856.

[43] A. J. Conejo, F. D. Galiana, I. Kockar, *Z-bus loss allocation*, IEEE Transactions on Power Systems 16.1 (2001): 105-110.

[44] K.T. Huynh, A. Barros, C. Berenguer, I. Castro, *A periodic inspection and replacement policy for systems subject to competing failure modes due to degradation and traumatic events*, Reliability Engineering and System Safety, 96.4 (2011): 497-508.

[45] J. Jacod, P. Protter, *Probability Essentials*, Springer (2004): 120.

[46] M. Compare, L. Bellani, E. Zio, *Availability model of a PHM-equipped component*, IEEE Transactions on Reliability, 66.2 (2017): 487 - 501.

Appendix A Complete framework

The complete procedure for the optimal allocation of PHM capabilities on a power transmission network is summarized in the following steps:

1. Estimation of the edges reliability when they are equipped with the different available PHM systems:
2. Optimization of $E^r[G]$ under the constraint of the limited budget using GA

The first step is performed by means of the following algorithm.

Data: Network edges failure rates, PHM system levels

for *each edge* $(m, n) \in E$ **do**

  for *each PHM system with performance level* $L_i, i \in \{1, \ldots, \Omega\}$ **do**

    Compute and store the reliability value $q^i_{m,n}$ of edge (m, n) with intrinsic reliability $u_{m,n}$ when equipped with PHM level L_i using the model developed in [20]

  end

end

To perform the second step, during GA iterations, $E^r[G]$ must be computed provided the particular allocation of PHM systems. The complete framework is also summarized in Figure 15.

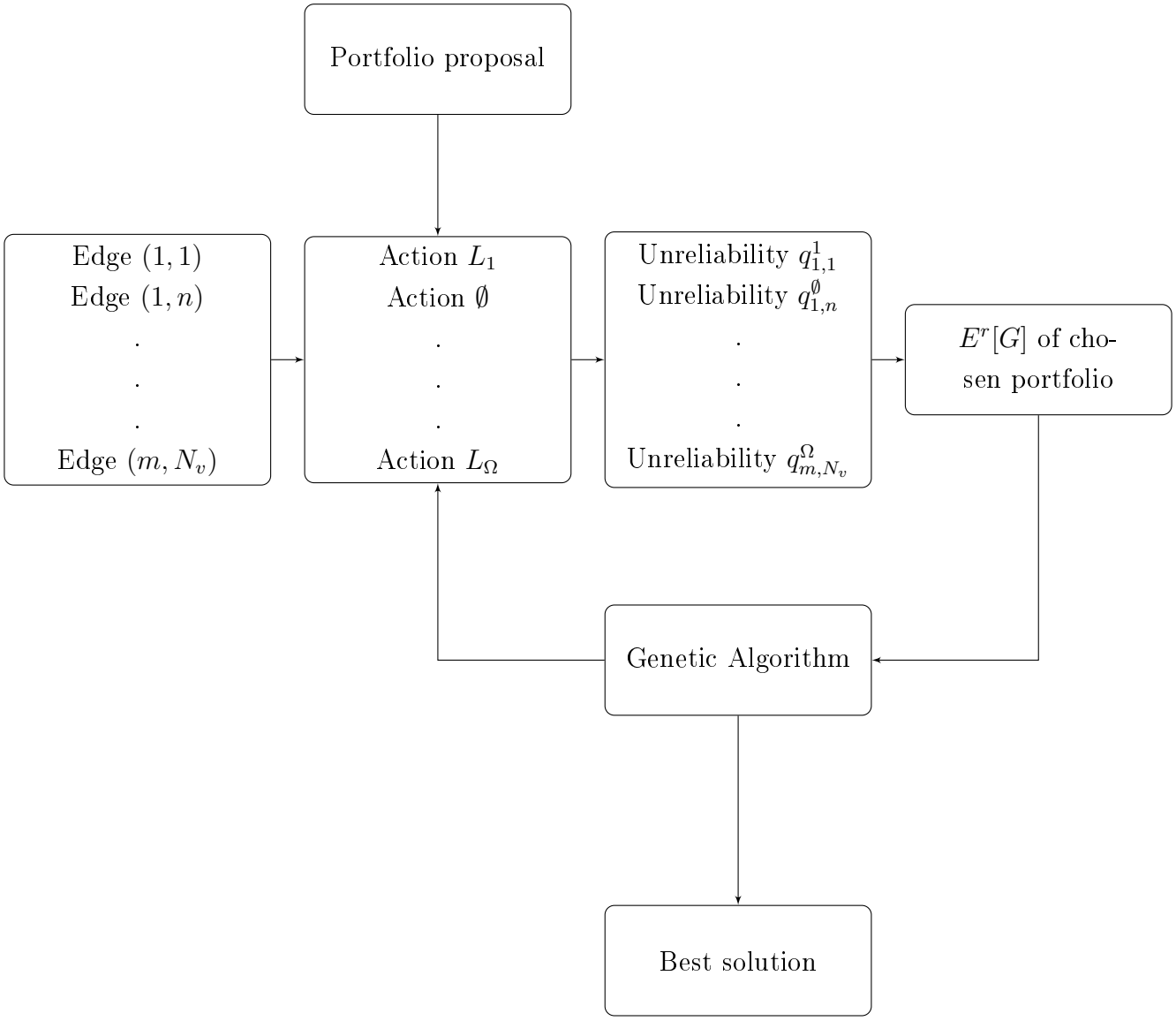

Figure 15: Summary of the proposed framework

Appendix B Reliability model

In this Section, we summarize the model proposed in [20] to estimate the reliability of a degrading element (component or system) of the network .

Based on the considerations and assumptions reported in Section 2, we can build the reliability model of a PHM-equipped component with estimated values $p^{\alpha}_{\lambda}, fn_{\lambda}, fp_{\lambda}$ of metrics $P^{\alpha}_{\lambda}, FN_{\lambda}, FP_{\lambda}$, respectively. To do this, we divide the time horizon into three regions (Figure 16):

1. The region in proximity of failure, i.e., Region 1, which is defined by the time indexes $k \geq N - h$ (i.e., equivalent time $\lambda = \frac{k}{N} \geq \frac{N-h}{N}$), such that $(1+\alpha)RUL_\lambda^* \leq h\Delta t$, where $RUL_\lambda^* = (N-h)\Delta t$. This is the same as $k \geq h^*$, where $h^* = \lfloor N - \frac{h}{1+\alpha} \rfloor$. Geometrically, this region corresponds to time values on the right of the intersection between the error upper bound line $(1+\alpha)RUL_\lambda^*$ and the horizontal line positioned at $RUL = h\Delta t$ (Figure 16). In this region, we can note that the alarm is required to be missing for $N - h^*$ consecutive times to have a failure. In this region, an alarm is missed only if the RUL over-estimation lies above the line $(1+\alpha)RUL_\lambda^*$, which happens with probability $(1 - P_\lambda^\alpha)FN_\lambda$. In this case, the predicted β percentile can be either above or below $h\Delta t$. As the available information is not enough to infer it and the stop is beneficial for the reliability of the component, we conservatively assume that in this case the component is not removed from operation.

2. The safe region, i.e., Region 2, which is indicated by time instants $k < k^*$, where k^* geometrically corresponds to the prediction most proximal to the intersection between the prediction error lower bound line $(1-\alpha)RUL_\lambda^*$ and the horizontal line at $RUL = h\Delta t$ (Figure 16). In this region, an over-estimation of RUL_λ^* leads to not stop the system before failure. This does not entail any risk of missing stops. On the contrary, an under-estimation of the RUL could lead to a component stop. In the risk-averse setting we are dealing with, the anticipated maintenance is beneficial for system reliability, as it avoids component failure. However, due to the lack of information and data, we cannot estimate the stop probability in this region based only on metric values. For this, we conservatively assume that in this left-most region the PHM system never stops the component: in this way we overcome our lack of knowledge assuming the worst possible case for the safety of the system (i.e., no stop).

3. The in-between region, i.e., Region 3, identified by $k^* \leq k < h^*$. We have to give account to the fact that some extreme cases may occur, where even if $\Pi_\lambda^\alpha = 1$, the $1-\beta$ probability mass and, thus, the $(1-\beta)^{th}$ percentile, is positioned above $h\Delta t$. For example, Figure 16 shows the situation where $t_{\lambda_1} = (N-h)\Delta t$ and all the β mass is concentrated between $RUL_\lambda^* = h\Delta t$ and α_λ^+. In this case, PHM will not advice to stop the component at t_{λ_1}. Thus, we conservatively assume that in this region the component does not undergo a maintenance action as long as $\Pi_\lambda^\alpha = 1$.
   On the contrary, when $\Pi_\lambda^\alpha = 0$, which occurs with probability $(1 - P_\lambda^\alpha)$, the following two possible situations can occur:

   - The $(1-\beta)^{th}$ percentile, Υ_λ, is smaller than $(1-\alpha)RUL_\lambda^*$. In this situation, which occurs with probability $(1-P_\lambda^\alpha)FP_\lambda$, even if we conservatively assume that the $(1-\beta)^{th}$ percentile takes the largest possible value (i.e., $\Upsilon_\lambda = (1-\alpha)RUL_\lambda^*$), the component is stopped as this time is smaller than $h\Delta t$.

- With probability $(1 - P_\lambda^\alpha)FN_\lambda$, Υ_λ will be above $(1+\alpha)RUL_\lambda^*$. In this situation, we will not stop the component.

To sum up, a conservative estimation of the stop probability in this time window is $(1 - P_\lambda^\alpha)FP_\lambda$ ([20]).

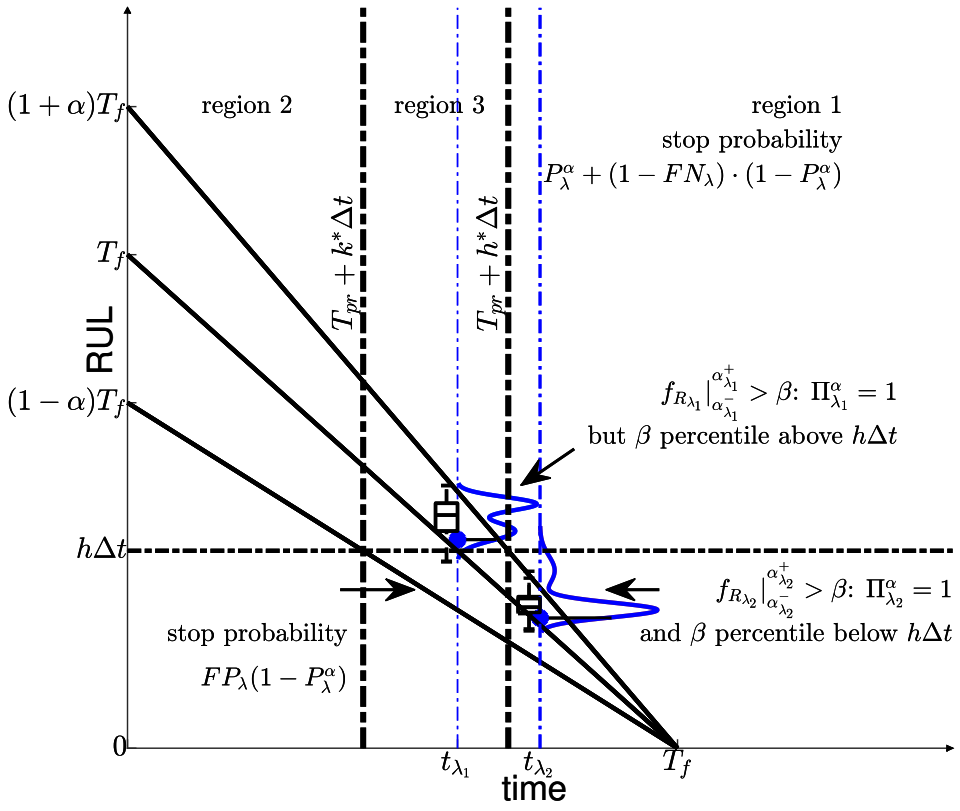

Figure 16: Regions partitioning the time horizon and examples of possible RUL predictions

The PHM-equipped component must be framed as a three-state system, the possible states being: *Working*, *Failed* and *Removed* (Figure 1); then, the component unreliability $u(t)$ represents the probability of having a transition from *Working* to *Failed* before time t, that is:

$$u(t) = \mathbb{P}(T_f \leq t \ \cap \ \text{system not removed before } t\,;\boldsymbol{\theta}) =$$

$$\mathbb{P}(T_f \leq t \mid \text{system not removed before } t\,;\boldsymbol{\theta}) \times \mathbb{P}(\text{system not removed before } t\,;\boldsymbol{\theta})$$

where $\boldsymbol{\theta}$ indicates the parameters determining the performance of the PHM system, which the unreliability depends on.

Accordingly, we derive $u(t)$ from the probabilistic transport kernel $K(t, Failed|t', s'; \boldsymbol{\theta})$, which is defined as the probability that the component makes the next transition between t and $t + dt$ towards state $Failed$ [28], provided that the previous transition has occurred at time t' and that the system had entered in state s'. However, in our case we assume that the component always starts at $t = 0$ in state $Working$. For this, we indicate the kernel as $K(t, Failed; \boldsymbol{\theta})$, without the conditioning event.
To calculate $K(t, Failed; \boldsymbol{\theta})$, we first calculate the failure transportation kernel given a realization δ from f_{DTD}:

$$K(t, Failed|\delta; \boldsymbol{\theta}) = \int_{t-\delta}^{t} f_{T_d}(\tau) f_{T_\phi}(t-\tau) d\tau + \int_{0}^{t-\delta} f_{T_d}(\tau) f_{T_\phi}(t-\tau) \prod_{k=k^*}^{h^*-1} [1 - (1 - p^{\alpha}_{\frac{k}{N}}) fp_{\frac{k}{N}}] \prod_{k=h^*}^{N-1} [(1 - p^{\alpha}_{\frac{k}{N}}) fn_{\frac{k}{N}}] d\tau \quad (11)$$

In words, given the detection delay δ, a failure occurs when one out of the following mutually exclusive and exhaustive conditions is satisfied, which are represented by the first and the second addend, respectively:

1. The component fails before PHM detects the initial failure state; this may happen in case the component fails abruptly and, thus, PHM is not capable of detecting this behavior.
2. PHM always fails to trigger an alarm until system failure; this happens after $T_{pr} + k^*\Delta t$ (i.e., the first prediction instant where a stopping decision should be made), with probability $1 - (1 - p^{\alpha}_{\frac{k}{N}}) fp_{\frac{k}{N}}$; then, from $T_{pr} + h^*\Delta t$ on, with probability $(1 - p^{\alpha}_{\frac{k}{N}}) fn_{\frac{k}{N}}$.

To remove the dependence from δ, we integrate Equation 11 over the distribution of DTD:

$$K(t, Failed; \boldsymbol{\theta}) = \int_{0}^{\infty} K(t, Failed|\delta; \boldsymbol{\theta}) f_{DTD}(\delta) d\delta \quad (12)$$

Generally speaking, the integral of $K(t, Failed)$ over the time interval $[t_1, t_2]$ gives the probability of failure in that time span [28]. Then, Equation 12 allows estimating the component unreliability as Equation 2.

Appendix C Sensitivity analysis of reliability model

In this Section, we report the results of the sensitivity analysis aimed at investigating the impact of the metric values FP_λ and FN_λ on the reliability of the PHM-equipped components. We do

not report the results of the sensitivity analysis with respect to P_λ^α as these are reported already in the case study: the three different performance levels L_1, L_2, L_3 exclusively depend on the P_λ^α value of the three different PHM systems under consideration.

In the next Tables, we report the results of the sensitivity analysis of the edge unreliability value at times $T = 1, 10$ with respect to constant values of $FP_\lambda = FP$ and $FN_\lambda = FN$. Namely, we consider the following three pairs of values: $FP = 0.1, FN = 0.9$, $FP = 0.2, FN = 0.8$ and $FP = 0.3, FN = 0.7$.

From the analysis of Tables 5-10, it emerges that when the value of P_λ^α is large (i.e., at performance value L_3) the unreliability of the network elements is not very sensitive to FP. On the contrary, at smaller values of P_λ^α (i.e., at performance value L_1), the unreliability of the network elements is more sensitive to FP.

$\lambda_{m,n}$ \ a	$\emptyset$	L_1	L_2	L_3
0.0105	0.9896	0.9951	0.9962	0.9965
0.5429	0.5811	0.7904	0.8312	0.8433
1.0858	0.3376	0.6513	0.7086	0.7261

Table 5: Reliability values $q_{m,n}$ of the edges corresponding to $a \in \mathcal{A}$, $T = 1$, $FN = 0.7, FP = 0.3$

$\lambda_{m,n}$ \ a	$\emptyset$	L_1	L_2	L_3
0.0105	0.9896	0.9940	0.9957	0.9961
0.5429	0.5811	0.7496	0.8090	0.8265
1.0858	0.3376	0.5882	0.6726	0.6972

Table 6: Reliability values $q_{m,n}$ of the edges corresponding to $a \in \mathcal{A}$, $T = 1$, $FN = 0.8, FP = 0.2$

$\lambda_{m,n}$ \ a	$\emptyset$	L_1	L_2	L_3
0.0105	0.9896	0.9928	0.9950	0.9956
0.5429	0.5811	0.6957	0.7815	0.8045
1.0858	0.3376	0.5075	0.6275	0.6614

Table 7: Reliability values $q_{m,n}$ of the edges corresponding to $a \in \mathcal{A}$, $T = 1$, $FN = 0.9, FP = 0.1$

$\lambda_{m,n}$ \ a	$\emptyset$	L_1	L_2	L_3
0.0105	0.9003	0.9678	0.9862	0.9915
0.5429	0.0044	0.6097	0.7575	0.8008
1.0858	0.0000	0.5429	0.6616	0.6968

Table 8: Reliability values $q_{m,n}$ of the edges corresponding to $a \in \mathcal{A}$, $T = 10$, $FN = 0.7, FP = 0.3$

$\lambda_{m,n}$ \ a	$\emptyset$	L_1	L_2	L_3
0.0105	0.9003	0.9552	0.9825	0.9898
0.5429	0.0044	0.4911	0.7148	0.7750
1.0858	0.0000	0.4360	0.6146	0.6639

Table 9: Reliability values $q_{m,n}$ of the edges corresponding to $a \in \mathcal{A}$, $T = 10$, $FN = 0.8, FP = 0.2$

$\lambda_{m,n}$ \ a	$\emptyset$	L_1	L_2	L_3
0.0105	0.9003	0.9387	0.9782	0.9880
0.5429	0.0044	0.3421	0.6611	0.7423
1.0858	0.0000	0.2997	0.5531	0.6211

Table 10: Reliability values $q_{m,n}$ of the edges corresponding to $a \in \mathcal{A}$, $T = 10$, $FN = 0.9, FP = 0.1$

Notice that the in Tables above we indicate the three available PHM systems as $\{L_1, L_2, L_3\}$. This is somewhat an abuse of notation: the systems have the same P_λ^α curves of the PHM systems considered in Section 5, but with values of FP_λ and FN_λ different from those presented in Section 5. The values of all the other parameters are set as in Section 5.